Appl Biochem Biotechnol
DOI 10.1007/s12010-017-2578-1

Development of an Amperometric Biosensor Platform for the Combined Determination of L-Malic, Fumaric, and L-Aspartic Acid

Désirée L. Röhlen[1] · **Johanna Pilas**[1] · **Michael J. Schöning**[1,2] · **Thorsten Selmer**[1]

Received: 12 June 2017 / Accepted: 2 August 2017

Abstract Three amperometric biosensors have been developed for the detection of L-malic acid, fumaric acid, and L-aspartic acid, all based on the combination of a malate-specific dehydrogenase (MDH, EC 1.1.1.37) and diaphorase (DIA, EC 1.8.1.4). The stepwise expansion of the malate platform with the enzymes fumarate hydratase (FH, EC 4.2.1.2) and aspartate ammonia-lyase (ASPA, EC 4.3.1.1) resulted in multi-enzyme reaction cascades and, thus, augmentation of the substrate spectrum of the sensors. Electrochemical measurements were carried out in presence of the cofactor β-nicotinamide adenine dinucleotide (NAD^+) and the redox mediator hexacyanoferrate (III) (HCFIII). The amperometric detection is mediated by oxidation of hexacyanoferrate (II) (HCFII) at an applied potential of + 0.3 V vs. Ag/AgCl. For each biosensor, optimum working conditions were defined by adjustment of cofactor concentrations, buffer pH, and immobilization procedure. Under these improved conditions, amperometric responses were linear up to 3.0 mM for L-malate and fumarate, respectively, with a corresponding sensitivity of 0.7 μA mM^{-1} (L-malate biosensor) and 0.4 μA mM^{-1} (fumarate biosensor). The L-aspartate detection system displayed a linear range of 1.0–10.0 mM with a sensitivity of 0.09 μA mM^{-1}. The sensor characteristics suggest that the developed platform provides a promising method for the detection and differentiation of the three substrates.

Keywords L-aspartic acid · L-malic acid · Fumaric acid · Amperometric biosensor · Enzyme · Fermentation

✉ Michael J. Schöning
schoening@fh-aachen.de

✉ Thorsten Selmer
selmer@fh-aachen.de

[1] Institute of Nano- and Biotechnologies (INB), FH Aachen, Heinrich-Mußmann-Straße 1, 52428 Jülich, Germany

[2] Peter Grünberg Institute (PGI-8), Forschungszentrum Jülich GmbH, 52425 Jülich, Germany

Published online: 02 September 2017

Introduction

L-malate, fumarate, and L-aspartate play a key role in the metabolism of all living organisms as intermediates in the tricarboxylic acid cycle (TCA) or amino acid metabolism. Besides their function in the energy metabolism, these dicarboxylic acids are also relevant in the food industry, where they serve as acidulants (fumarate, L-malate) or as component for the synthesis of the artificial sweetener aspartame (L-aspartate). Moreover, they have also been recognized as important feedstocks for the manufacturing of biodegradable polymers [1]. Due to the increasing demand on renewable supplies, there is a growing interest in the production of organic acids via biosynthetic pathways, including enzymatic conversion and direct fermentation of sugars [2, 3]. Besides chemical synthesis, large-scale production of malic acid can be achieved by hydration of fumaric acid to malic acid catalyzed by fumarase [4, 5] or by fungal fermentation of sugars [6, 7]. Fumaric acid is mainly obtained by catalytic isomerization of petroleum-based maleic anhydride. Fermentative production is usually carried out with *Rhizopus oryzae* [8, 9]. The production of the amino acid L-aspartate is based on the enzymatic conversion by an aspartate ammonia-lyase (ASPA), which catalyzes the amination of fumaric acid, resulting in the formation of L-aspartic acid. Either partially purified enzymes [10] or whole bacterial cells overexpressing the ASPA gene have been described in literature for the production of L-aspartate [11–14].

During fermentation, the continuous monitoring is necessary for the efficient acid production. Quantification of the acids is usually realized by high-performance liquid chromatography (HPLC) or ion-exchange chromatography. However, these methods are generally expensive and time-consuming and require an elaborate sample pretreatment. Although several electrochemical biosensors for the specific detection of L-malic acid [15–20], fumaric acid [21, 22] and L-aspartic acid [23–27] have been reported in the literature; no system has yet been developed for the combined detection of these three metabolic intermediates.

The present work describes the development of three amperometric biosensors, all of which build on each other and permit the detection of L-malate, fumarate, and L-aspartate simultaneously. The modular system is based on the combination of malate dehydrogenase (MDH) and diaphorase (DIA), as previously described in other studies [15, 16]. The determination of L-malate is achieved by enzymatic conversion of the substrate into oxaloacetate (OAA) with simultaneous reduction of the cofactor NAD^+, catalyzed by MDH (Fig.1, reaction a). In the next step, the reduced β-nicotinamide adenine dinucleotide (NADH) is regenerated by the DIA, resulting in the reduction of the redox mediator hexacyanoferrate (III). Finally, the amperometric detection is mediated by the oxidation of hexacyanoferrate (II) at an applied potential of + 0.3 V vs. Ag/AgCl. The extension of the system for the detection of fumarate is realized by combination of the malate sensor with a fumarate hydratase (FH). This enzyme

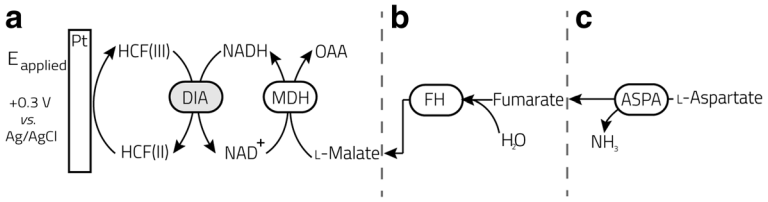

Fig. 1 Detection principle for the three amperometric biosensors. Illustration of the enzymatic reactions used for the detection of L-malate (a), fumarate (b), and L-aspartate (c)

catalyzes the hydration of the carbon-double bond of fumarate to yield L-malate (Fig. 1, reaction b). The aspartate sensor is formed by addition of the ASPA to the system for fumarate detection (Fig. 1, reaction c). In this reaction, L-aspartate is deaminated into fumarate and, thus, serves as substrate for the further steps of the enzyme cascade.

In this work, we present the development and optimization of an extended malate platform for the combined quantification of the analytes. This system enables the rapid determination and differentiation of the three individual substrates and is therefore suitable for a broad range of applications, including the monitoring of fermentative or enzymatic production and also the determination in food or beverage samples. Due to their crucial role in energy metabolism, the monitoring of these organic acids would also be advantageous for other applications involving microbial processes, for example in the biogas process. In addition to several key parameters such as acetate, propionate, and lactate, the constant observation of various other metabolites may lead to an improved understanding of the events that occur in a biogas reactor.

Experimental

Materials

Diaphorase from *Clostridium kluyveri* (DIA, EC 1.8.1.4) and fumarate hydratase from porcine heart (FH, EC 4.2.1.2) were purchased from Sigma Aldrich Co. (St. Louis, MO, USA). Malate dehydrogenase from porcine heart (MDH, EC 1.1.1.37) was acquired from Merck (Darmstadt, Germany) as well as the substrates L-aspartic acid and di-sodium fumarate. Glycerol, Tris, KH_2PO_4 and K_2HPO_4, $MgCl_2$, glycine, and Roti-Nanoquant were obtained from Roth (Karlsruhe, Germany). Nicotinamide adenine dinucleotide (NAD^+) was supplied by Applichem (Darmstadt, Germany). Bovine serum albumin (BSA), glutaraldehyde solution (GA) (25%), di-sodium L-malate, and potassium hexacyanoferrate (III) were also purchased from Sigma Aldrich. GeneJET plasmid and polymerase chain reaction (PCR) purification kits, Phusion DNA Polymerase, T4 Ligase, and restriction enzymes were supplied by Fisher scientific (Schwerte, Germany).

Gene Expression and Biomass Production

The aspartase gene (*aspA*) was amplified from chromosomal DNA (deoxyribonucleic acid) of *Escherichia coli* DSM30083^T by PCR with simultaneous elimination of an internal recognition site for *Lgu*I. Purified PCR products were analyzed by chip electrophoresis (MCE-202 MultiNA; Shimadzu, Duisburg, Germany) and further cloned into a pENTRY vector (IBA, Göttingen, Germany). *E. coli* DH5α competent cells were transformed with the resultant plasmid. The donor vector was extracted with GeneJET plasmid purification kit followed by subcloning into a StarGate Acceptor Vector (IBA, Göttingen, Germany), containing a C-terminal-fused Strep-tag [28]. The correct nucleotide sequence of the *aspA* insert was confirmed by sequencing (Eurofins Genomics, Ebersberg, Germany).

Gene expression and biomass production were performed using *E. coli* Bl21 (DE3) cells (Merck, Darmstadt, Germany), harboring the expression plasmid. Freshly transformed cells were grown overnight in LB (Luria-Bertani) medium (100 ml) with 50 μg/ml carbenicillin at 28 °C. On the next day, the culture was inoculated to 500 ml of the same medium and gene expression was induced with anhydrotetracycline (200 ng/ml) at an optical density (OD_{578nm})

of 0.5–0.7. After incubation for 2 h at 28 °C, the cells were harvested by centrifugation and washed with 50 mM Tris buffer (pH 7.4) containing 150 mM NaCl. Cell pellets were stored at −80 °C until used for protein purification.

Protein Purification

Aspartase was purified by affinity chromatography using a Strep-Tactin Macroprep column (IBA GmbH, Göttingen, Germany). The collected cells were suspended in 25 ml of equilibration buffer (100 mM Tris-buffer pH 8.0, 150 mM NaCl, 2.0 mM $MgCl_2$) and disrupted by sonication using a Bandelin Sonopuls Homogenizer (Bandelin electronic, Berlin, Germany). Cell debris was removed by ultracentrifugation at 100,000×*g* for 1 h, and the clear supernatant was loaded onto the equilibrated column. The protein was eluted in aforementioned buffer, supplemented with 2.5 mM d-desthiobiotin. Fractions containing purified aspartase were pooled and concentrated by ultrafiltration. Ten percent glycerol was added to the protein solution followed by storage at −20 °C. The protein concentration was estimated by using Roti-Nanoquant reagent (Roth) according to the manufacturer's protocol with BSA as standard. The purity and molecular mass was checked by sodium dodecyl sulfate polyacrylamide gel electrophoresis (SDS-PAGE). The storage buffer was exchanged with 100 mM phosphate buffer (pH 8.0) containing 2.0 mM $MgCl_2$ prior to enzyme immobilization.

Enzyme Activity Measurements

Aspartase activity was determined spectrophotometrically according to Asano, Kira and Yokozeki (2004) [29]. The assay mixture contained 100 mM Tris-HCl buffer (pH 8.5), supplemented with 2 mM $MgCl_2$ and 100 mM L-aspartate in a total volume of 1 ml. The reaction was started by addition of the enzyme, and the formation of fumarate was monitored for 3 min at 30 °C. The resulting absorbance increase at 240 nm was measured using an Ultrospec 2100 pro spectrophotometer (Amersham Biosciences, UK). A molar extinction coefficient of $\varepsilon_{240nm} = 2.53\ mM^{-1}\ cm^{-1}$ was used to calculate enzyme activities.

Sensor Preparation

The biosensor array chips were fabricated from a p-Si wafer by thin-film technology and photolithographic techniques according to Pilas et al. (2015) [30]. Furthermore, the sensor, consisting of five platinum working electrodes (Ø = 2 mm), was passivated with a 20-μm thick layer of SU-8 photoresist (SU-8 25, micro resist technology GmbH) [31]. A schematic representation of sensor layout and cross-section are shown in Fig. 2. Prior enzyme immobilization, the electrode surface was cleaned electrochemically in a solution of 0.5 M aqueous H_2SO_4 by applying an anodic current of + 2.0 V vs. Ag/AgCl for 2 min and subsequent potential cycling (− 0.2 V to + 1.4 V at a scan rate of 100 mV s^{-1}) was executed until constant voltammograms were obtained [32].

Enzyme Immobilization

The preparation of enzyme membranes was carried out by crosslinking the proteins with the amine-reactive agent GA. For the construction of the L-malate biosensor, MDH and DIA were dissolved in 0.1 M phosphate buffer pH 8.0 and added with 2.0% of the inert protein BSA.

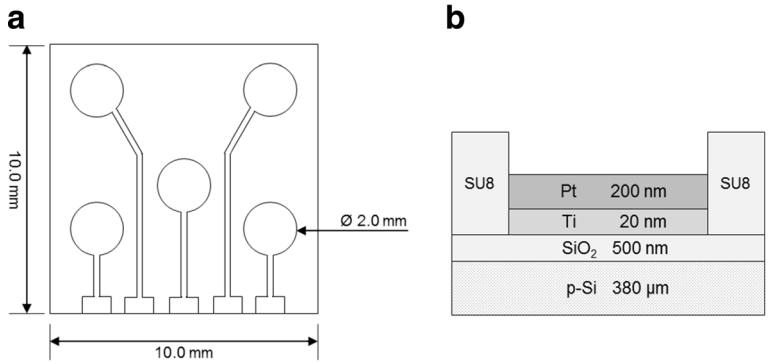

Fig. 2 Schematic sensor layout with five working electrodes (**a**) and cross-section of the sensor chip (**b**)

Subsequently, 0.4% GA was added and 1.5 µl of this mixture was applied to the electrode surface via drop-coating. After drying at room temperature in air for 30 min, the sensor was stored for at least 12 h at 4 °C until use. 1.5 units (U) per electrode MDH and 2.0 U/electrode DIA were used for fabrication of the malate sensor, and the amounts of these two enzymes were kept constant for the following sensors. The fumarate sensor employs an enzyme layer containing MDH (1.5 U), DIA (2.0 U), BSA (2.0%), and GA (0.4 vol%) and fumarate hydratase (1.5 U). The L-aspartate sensor contains aforementioned amounts of the crosslinking agent and the enzymes DIA, MDH, and FH, and additionally, 1.48 U of ASPA. Due to the limited volume that can be applied to the electrode, the concentration of BSA was reduced to 1.59%.

Amperometric Detection

Electrochemical studies were performed by using a potentiostat (PalmSens, Palm Instruments BV) coupled with an eight-channel multiplexer (MUX8, Palm Instruments BV). Amperometric measurements were carried out in a conventional three-electrode setup with a platinum counter electrode (Ø = 7.5 mm), an Ag/AgCl reference electrode, and the biosensor chip. After an equilibration phase (10 min) of the sensors in the buffer solution, chronoamperometric measurements were conducted at an applied potential of + 0.3 V vs. Ag/AgCl with constant stirring. Unless otherwise stated, all amperometric measurements were carried out in 0.1 M glycine buffer (pH 9.0 for the malate biosensor and pH 8.5 for the fumarate and aspartate biosensor) supplemented with 2.5 mM NAD^+, 5.0 mM hexacyanoferrate (III), and 5.0 mM $MgCl_2$ in a total volume of 12 ml. The calibration curves of the three biosensors were determined by successive addition of a stock solution of the respective substrate. All experiments were carried out at room temperature.

Optimization Procedure

Optimization procedures were performed with respect to the amount of GA in the immobilization process along with individual components of the working solution. Due to its arrangement with five individual working electrodes, the proposed sensor layout enables parallel measurements at constant experimental conditions. Thus,

optimization procedures were usually carried out by simultaneous measurements with multiple electrodes, all equally prepared for the detection of the individual analytes. The optimization of the malate sensor was executed in 0.1 M glycine buffer (pH 9.0) with 1.0 mM L-malate. The fumarate sensor was usually employed in 0.1 M glycine buffer (pH 8.5), containing 1.0 mM fumarate, and the same buffer was used for the aspartate sensor, supplemented with 5.0 mM L-aspartate. For the optimization of the immobilization procedure, various concentrations of glutaraldehyde (0.2–1.0 vol% in 10 vol% glycerol) were used for the preparation of the enzyme layer with fixed concentrations of enzyme and BSA. Different buffer systems with a concentration of 0.1 M were used for pH optimization. MES-buffer was used for pH 5.5–6.5, phosphate buffer was used for pH 7.0–8.0, and glycine buffer was used for alkaline pH ranges above pH 8.5. In addition, the most suitable concentration of the cofactor NAD^+ (0.25–3.5 mM) was determined and the concentration of the redox mediator hexacyanoferrate (III) (0.25–3.5 mM) was also adjusted.

The relative response (%) was calculated from the obtained current signals in relation to the maximum observed signal response (100%), which allows a better comparability between the three different biosensors.

Results and Discussion

Optimization of Experimental Conditions

Effect of Glutaraldehyde Concentration on the Biosensor Response

Among the various existing immobilization procedures, the use of the crosslinker glutaraldehyde is a popular method due to its efficiency and versatility [33]. The enzymes are covalently linked to the aldehydes via their amine groups, resulting in the formation of a chemically and thermally stable enzyme layer. In order to ensure both, the formation of a stable enzyme layer and the maintenance of the catalytic activity, various considerations have to be taken into account. Since the treatment with glutaraldehyde can result in a conformational change of the protein and loss of activity, the most suitable concentration of the crosslinking agent has to be found, in order to minimize the impairment of the enzyme activity. In addition, the use of the inert protein BSA may also have a stabilizing effect on the enzyme structure, due to its high lysine content [34].

The appropriate GA amount for the three different biosensors was selected by varying the concentration of the crosslinker in the immobilization mixture in a range of 0.2 to 1.0% (*v*/*v*). For this purpose, each of the five working electrodes of one sensor was coated with a specific glutaraldehyde concentration and equal amounts of enzymes and BSA.

The impact of the crosslinker on the enzyme activities was investigated by comparing the current generated after the addition of the specific substrate. The results are depicted in Fig. 3a–c. The malate sensor displays a maximal signal response at 0.4% of GA while the current obtained gradually decreases with rising GA concentrations, indicating an inactivation of the enzyme (Fig. 3a). When GA is in excess, multiple crosslinking events can occur, which may lead to conformational changes in the enzyme structure, thus, affecting the catalytic activity [35]. Moreover, a concentration

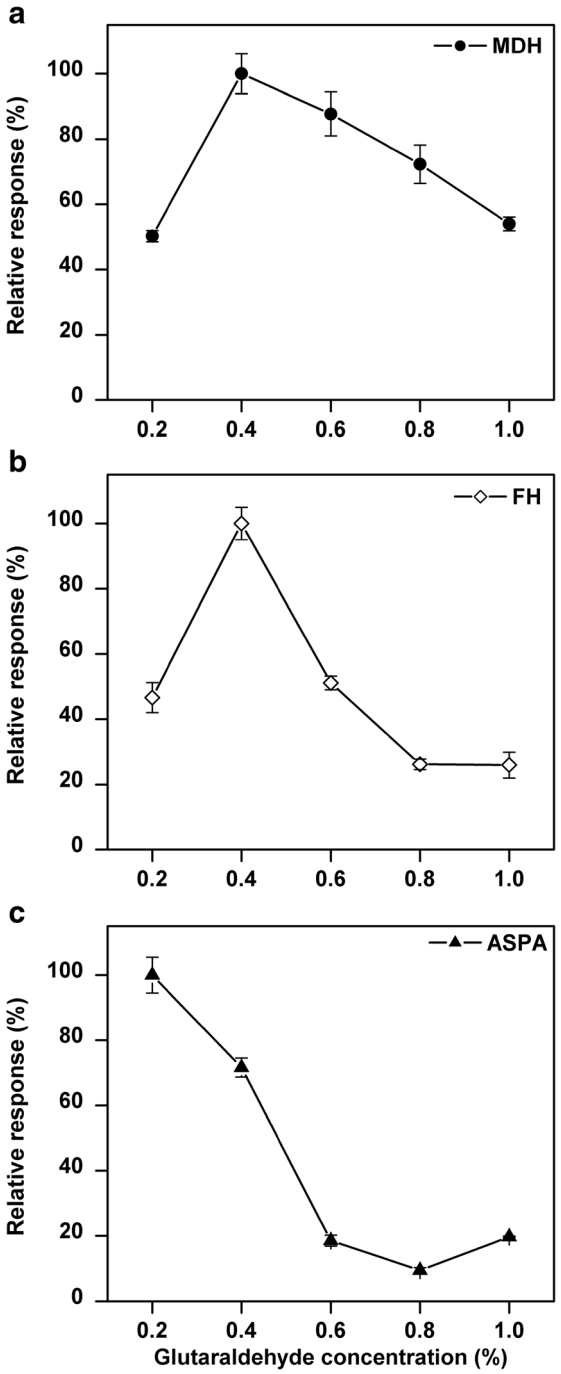

Fig. 3 Effect of the glutaraldehyde concentration on the amperometric responses of the three biosensors, (**a**) malate biosensor (MDH), (**b**) fumarate biosensor (FH), and (**c**) aspartate biosensor (ASPA), (Mean ± SD, $n = 2$). Experimental conditions 5.0 mM HCF (III), 2.5 mM NAD^+, 5.0 mM $MgCl_2$, 1.0 mM (L-malate and fumarate, respectively), and 5.0 mM (L-aspartate) substrate in 0.10 M glycine buffer pH 8.5 (for measurements with fumarate and aspartate biosensor) and pH 9.0 (malate biosensor)

of 0.2% also showed a detrimental effect on the signal response. Apparently, the amount of glutaraldehyde added to the enzyme mixture was not sufficient to immobilize all the proteins on the sensor surface, consequently, resulting in a reduced signal response.

The fumarate sensor showed a response towards increasing glutaraldehyde concentrations and was significantly stronger inhibited than the malate sensor at concentrations above 0.4% (Fig. 3b). This suggests that fumarase is more sensitive to the action of GA than MDH and DIA.

The L-aspartate sensor exhibits a slightly different behavior compared to the two sensors mentioned above (Fig. 3c). Here, the highest signal response was observed with the lowest concentration of glutaraldehyde (0.2%) and any increase in the glutaraldehyde concentration caused a decline in the current. This suggests that the aspartase is the most susceptible enzyme with respect to inactivation by the crosslinker as compared to the other enzymes used on the biosensors. Although the L-aspartate sensor showed maximal activity with 0.2% glutaraldehyde, the mixture did not polymerize into a stable enzyme layer and was washed out during the measurements. Therefore, a glutaraldehyde concentration of 0.4% was considered to be the most suitable for the aspartate sensor, as well as for the other two biosensors.

Effect of pH on the Amperometric Response

The evaluation of the optimum pH in a working buffer is a critical factor for the improvement of the biosensor response, especially in a system consisting of multiple enzymes, each of which displays its distinct pH optimum. Hence, the effect of different pH values on the sensor performance was investigated by measuring the signal response of the sensors in different buffer systems between pH 5.5 and 10.5 after addition of the substrate (1.0 mM L-malate, 1.0 mM fumarate, and 5.0 mM L-aspartate, respectively, for the corresponding biosensor). The results for the three biosensors are depicted in Fig. 4a–c.

As expected, the malate sensor showed a maximum signal response at an alkaline pH range (Fig. 4a) and loses its activity rapidly at pH values below 7.5. This is due to the chemical equilibrium of the MDH catalyzed, which favors oxaloacetate reduction at low and neutral pH values. The pH optimum of the DIA is in a range of pH 7.0 [36] and might influence the working range of the system as well. In combination, the best result for the malate sensor was obtained at a pH of 9.0, which is consistent with the results of previous studies of DIA-based malate sensor [16].

The fumarate biosensor exhibited maximal response at pH 8.5 (Fig. 4b), which deviates strongly from the pH optimum (pH 6.95) of the free enzyme [37]. However, in the case of the immobilized enzyme, the resulting current is generated by the reaction of the DIA/MDH enzyme couple and consequently, the pH optimum is apparently shifted in favor for this reaction when the fumarase is provided in excess.

The aspartate sensor showed a pH optimum between 7.5 and 8.5 with a maximum value at pH 8.5 (Fig. 4c), which corresponds to data reported in the literature [38] for the free enzyme. Values higher than pH 9.0 resulted in a complete loss of aspartase enzyme activity, which was also recognized by Fatibello-Filho, Suleiman and Guibault [27], using a potentiometric electrode with immobilized aspartase from *Hafnia alvei*.

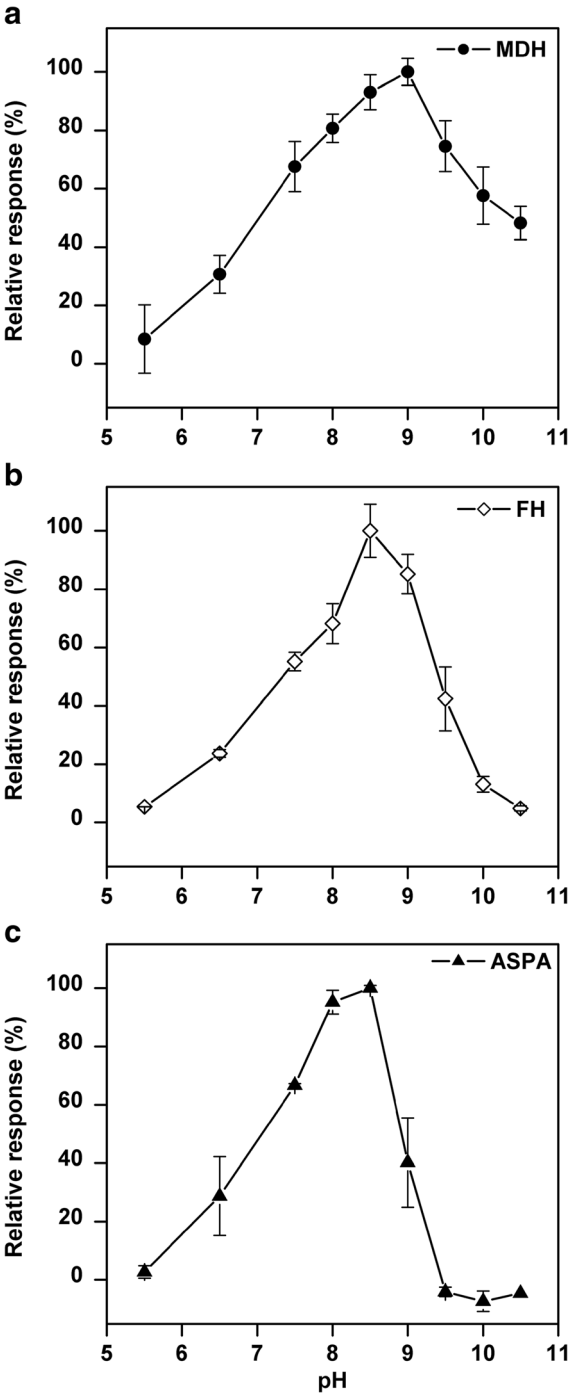

Fig. 4 Effect of pH on the signal response of (**a**) malate biosensor (MDH), (**b**) fumarate biosensor (FH), and (**c**) aspartate biosensor (ASPA). Signal responses were determined at pH 5.5 to 10.5 with constant concentrations of 2.5 mM NAD^+, 5.0 mM hexacyanoferrate (III), 5.0 mM $MgCl_2$, 1.0 mM (L-malate and fumarate, respectively), and 5.0 mM (L-aspartate) substrate. (Mean ± SD, $n = 3$)

In alkaline conditions, the enzyme was observed to have an absolute requirement for divalent metal ions [39]. Accordingly, the concentration of Mg^{2+} (5.0 mM) provided in the working buffer was increased to 10.0 mM, but this did not increase enzyme activity (data not shown).

Optimization of Cofactor Concentrations

Apart from the pH, the buffer composition was optimized with regard to NAD^+ and hexacyanoferrate (III) concentration, in order to avoid excessive cofactor consumption. Standard conditions of the NAD^+ optimization procedure for the three different biosensors were 5.0 mM hexacyanoferrate (III) and 5.0 mM L-aspartate, 1.0 mM fumarate, and 1.0 mM L-malate, respectively, in a buffer (0.1 M) at ideal pH conditions (see experimental section for details). Amperometric measurements were performed with successive addition of NAD^+ until no further signal increase was observed. Figure 5 presents the behavior of the three biosensors towards increasing concentrations of NAD^+. The current response shows an increase with stepwise titration of NAD^+ from 0.25 to 2.5 mM. Above 2.5 mM NAD^+, no significant increase in the response occurred. All three biosensors appeared to respond in a similar manner and were saturated at a concentration of 2.5 mM NAD^+.

In addition to optimum NAD^+ concentration, the most suitable concentrations of the redox mediator HCF (III) in the working solution were also determined for the three biosensors. Adjustment of the HCF (III) concentration was carried out in a range of 0.25 to 3.5 mM. As can be seen in Fig. 6, saturation levels of the mediator were observed at a concentration of 1.5 mM (fumarate and aspartate biosensor) and 2.0 mM (malate biosensor).

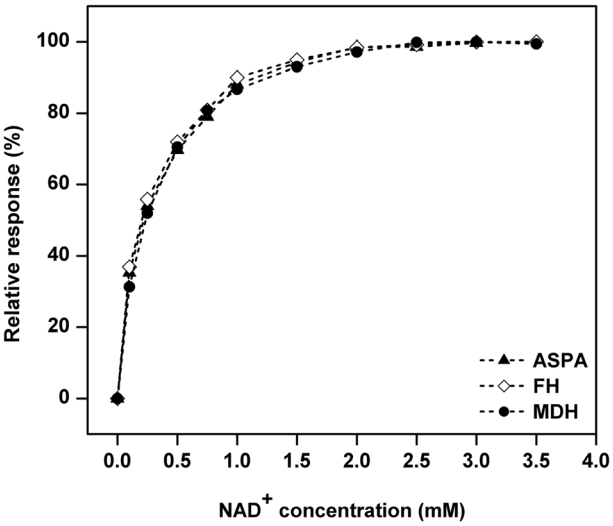

Fig. 5 Effect of NAD^+ concentration on the amperometric response of the biosensor for malate (MDH, filled circles), fumarate (FH, diamonds), and aspartate (ASPA, filled triangles) detection. Determination of the signal response upon successive addition of NAD^+ (0.25–3.5 mM) in 0.1 M glycine buffer pH 8.5 (fumarate and aspartate biosensor) and pH 9.0 (malate biosensor), supplemented with 5.0 mM HCF (III), 5.0 mM $MgCl_2$, 1.0 mM (L-malate and fumarate, respectively), and 5.0 mM (L-aspartate) substrate

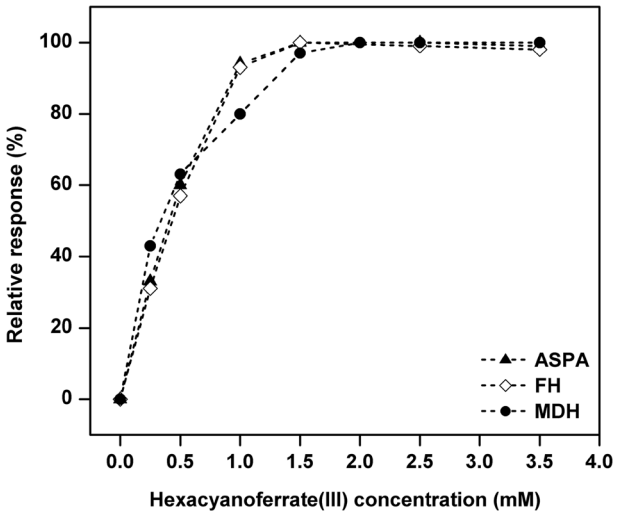

Fig. 6 Effect of hexacyanoferrate (III) concentration on the amperometric response of the biosensor for malate (MDH, filled circles), fumarate (FH, diamonds), and aspartate (ASPA, filled triangles) detection. Determination of the signal response upon successive addition of HCF (III) (0.25–3.5 mM) in 0.1 M glycine buffer pH 8.5 (fumarate and aspartate biosensor) and pH 9.0 (malate biosensor), supplemented with 2.5 mM NAD^+, 5.0 mM $MgCl_2$, 1.0 mM L-malate and fumarate, respectively), and 5.0 mM L-aspartate) substrate

The consistency of the results of the three biosensors is not particularly surprising. Since the MDH/DIA enzyme couple is responsible for the consumption of NAD^+ (MDH) and the reduction of hexacyanoferrate (III) (DIA), the saturation levels highly depend on the activity of those two enzymes. Apparently, the presence of FH and ASPA is negligible and has no distinct effect on cofactor concentrations.

Characterization of the Biosensors

The performance of the three different biosensors for the detection of L-malate, fumarate, and L-aspartate was evaluated in regard to sensitivity, linear detection range, and limit of detection. Calibration curves of the sensors were obtained by successive addition of the corresponding analyte to the buffer solution. Exemplarily, the steady-state current response of the aspartate sensor to stepwise increasing concentrations of L-aspartate is shown in Fig. 7. Based on the enzyme cascade of the aspartate sensor (Fig. 1), the current increase is caused by the anodic oxidation of HCF (II), the product of the DIA reaction. The inset to Fig. 7 shows the resulting calibration curve of the current response to the substrate concentration in a range from 0.5 to 17.5 mM L-aspartate. The sensor covered a linear detection range from 1.0 to 10.0 mM (Fig. 8c), which is remarkably wider than that of amperometric aspartate sensors developed by Villarta et al. (1–200 μM) [23] and Palleschi et al. (5–200 μM) [24] using aspartate transaminase and glutamate oxidase. However, better performances were achieved with potentiometric aspartate sensors, based on aspartase and subsequent ammonia detection. Those sensors showed a linear range of 0.7–20 mM [27] and 1.9–24 mM [25] but suffered from long response times (4–5 and 3 min). Compared to that, the sensor described in this paper has shorter response time of approximately 60 s, indicating a rapid conversion of the substrate. The corresponding sensitivity of the sensor was 0.09 μA mM^{-1} (R = 0.997) with a detection limit of 0.068 mM (S/N = 3).

The linear detection range of the fumarate biosensor was observed in a range of 0.1–3.0 mM (Fig. 8b). The sensitivity was 0.4 μA mM^{-1} (R = 0.996) with a detection limit of 0.026 mM. A further enzymatic approach within a flow-injection system, using fumarase and malate dehydrogenase in combination with spectrofluometric detection of NADH was described by Rhee and Sohn [40]. In this study, a linear working range of 0.43–2.6 and 0.86–5.2 mM was obtained, which is in good agreement with our results. Other biosensing systems for the detection of fumarate were prepared using microbial cells, like *Shewanella oneidensis* [22] or *Geobacter sulfurreducens* [21] with a linear range of 2 μM–10 mM and 0–3.2 mM, respectively.

The L-malate biosensor showed a sensitivity of 0.7 μA mM^{-1} (R = 0.997) with a linear detection limit of 0.011 mM. A linear relationship between current increase and the L-malate concentration was observed in range of 0.025–3.0 mM (Fig. 8a). Similar approaches using DIA and MDH showed a more narrow linear range of 0.01–0.61 mM [16] and 0.73 μM–0.035 mM [15] in comparison to our results.

In Table 1, the characteristics of the three biosensors are summarized. As can be seen, the aspartate sensor shows a significantly lower sensitivity compared to the both other biosensors. Since more enzyme molecules are added with each extension of the sensor, this results in a thicker enzyme matrix and thus a higher diffusion barrier for the analytes. Moreover, the results from the optimization of the immobilization process indicate a severe impairment of the aspartase activity by glutaraldehyde. Since GA is known to react with the ε-amino groups of lysines, this phenomenon might lead to a conformational change of the protein structure during polymerization. As observed by Saribas, Schindler and Viola (1993) [41], mutation of a lysine

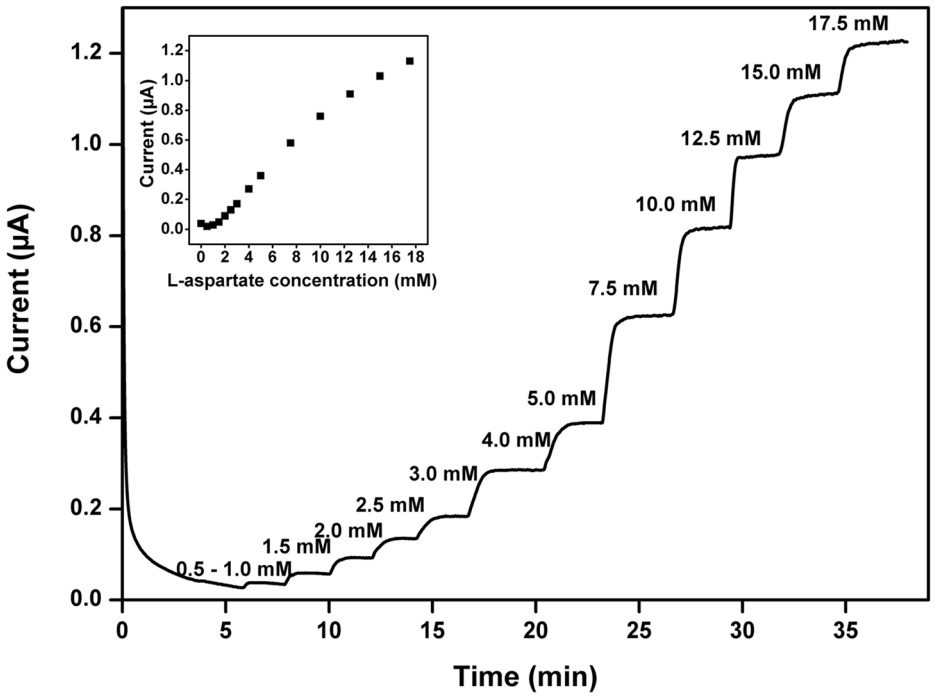

Fig. 7 Steady-state amperometric response of the aspartate sensor upon successive addition of L-aspartate (0.5–17.5 mM) in 0.1 M glycine buffer (pH 8.5) at an applied potential of + 0.3 V vs. Ag/AgCl. Inset: corresponding calibration curve of the current response to the L-aspartate concentration

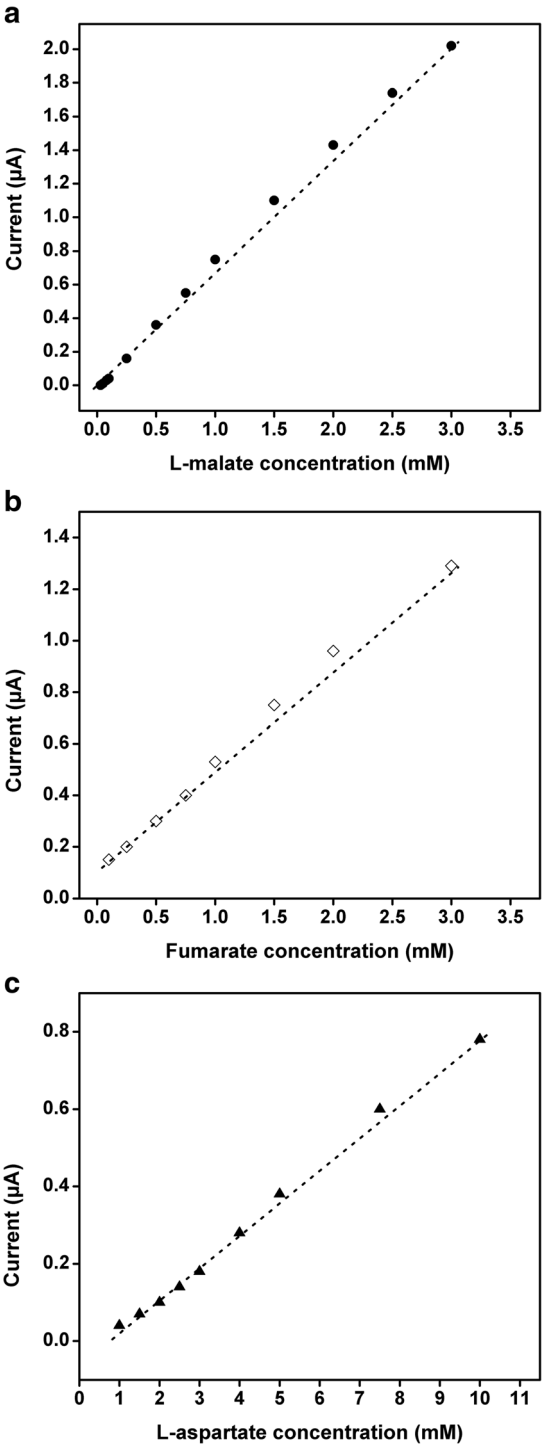

Fig. 8 Linear calibration curves of the three biosensors for the detection of (**a**) L-malate, (**b**) fumarate, and (**c**) L-aspartate sensor

Table 1 Typical sensor characteristics of the three biosensors

Sensor	Sensitivity ($\mu A\ mM^{-1}$)	Linear range (mM)	Detection limit (mM)
L-malate	0.7 ± 0.068	0.025–3.0	0.011
Fumarate	0.4 ± 0.065	0.1–3.0	0.026
L-aspartate	0.09 ± 0.013	1.0–10.0	0.068

residue in the suspected active site of the enzyme yielded in a significant decrease in the substrate binding activity. Thus, the use of GA for immobilization could have a significant adverse effect on the catalytic activity of the enzyme compared to proteins with low lysine content or without a catalytic function of the amino acid. Currently, the stabilizing effect of different BSA concentrations on the enzyme activity is investigated. Nevertheless, the performance of the sensor could be successfully improved by the individual optimization steps. Compared to previous experiments prior to optimization, the sensitivity was increased from 0.026 $\mu A\ mM^{-1}$ (data not shown) to 0.08 $\mu A\ mM^{-1}$ and the linear range was expanded from 4.5–7.0 to 1.0–10.0 mM. The beneficial effect of the optimization procedure was also clearly visible in the sensor performance of the other two sensors.

Conclusion

In this work, we have successfully demonstrated the extension of a bi-enzymatic biosensor, based on malate dehydrogenase and diaphorase, with the stepwise addition of the enzymes fumarase and aspartase. As a result, two novel amperometric detection systems for the important metabolic intermediates fumarate and aspartate have been developed. All three biosensors were optimized with regard to buffer composition and immobilization procedure and were characterized according to their sensitivity and linear detection range. All of them showed satisfactory operational characteristic with equal or improved linear detection ranges compared to previous studies in literature. Further work will focus on investigations on the interference with other substrates and improvement of the stability. The simultaneous quantification of the three analytes is an important step towards facilitating the monitoring of metabolic processes. Therefore, the combination of the three systems on one sensor array for the creation of a multi-analyte biosensing system is intended with subsequent evaluation of the system in biological samples.

Funding This work is financially supported by the German Federal Ministry of Food and Agriculture (BMEL) and the Agency of Renewable Resources (FNR) (FKZ: 22006613).

References

1. Werpy, T. and Petersen, G. (2004) Top value added chemicals from biomass: volume I—results of screening for potential candidates from sugars and synthesis gas, United States.
2. Goldberg, I., Rokem, J. S., & Pines, O. (2006). Organic acids: old metabolites, new themes. *Journal of Chemical Technology and Biotechnology, 81*, 1601–1611.
3. Magnuson, J. K., & Lasure, L. L. (2004). Organic acid production by filamentous fungi. In J. S. Tkacz & L. Lange (Eds.), *Advances in fungal biotechnology for industry, agriculture and medicine* (pp. 307–340). New York: Kluwer Academic/Plenum Publishers.

4. Presečki, A. V., Zelić, B., & Vasić-Rački, Đ. (2009). Modeling of continuous L-malic acid production by porcine heart fumarase and fumarase in yeast cells. *Chemical and Biochemical Engineering Quarterly, 23*, 519–525.
5. Almuaibed, A. M. (2001). Microscale on-line production and determination of malic acid using flow injection analysis, immobilized fumarase and malate dehydrogenase with chemiluminescence detection. *Analytica Chimica Acta, 428*, 1–6.
6. Zambanini, T., Hosseinpour Tehrani, H., Geiser, E., Sonntag, C. K., Buescher, J. M., Meurer, G., Wierckx, N., & Blank, L. M. (2017). Metabolic engineering of *Ustilago trichophora* TZ1 for improved malic acid production. *Metab. Eng. Commun., 4*, 12–21.
7. West, T. P. (2017). Microbial production of malic acid from biofuel-related coproducts and biomass. *Fermentation, 3*, 14–23.
8. Roa Engel, C., van Gulik, W., Marang, L., van der Wielen, L., & Straathof, A. (2011). Development of a low pH fermentation strategy for fumaric acid production by *Rhizopus oryzae*. *Enzyme and Microbial Technology, 48*, 37–47.
9. Zhou, Y., Du, J., & Tsao, G. (2002). Comparison of fumaric acid production by *Rhizopus oryzae* using different neutralizing agents. *Bioprocess and Biosystems Engineering, 25*, 179–181.
10. Cárdenas-Fernández, M., López, C., Álvaro, G., & López-Santín, J. (2012). Immobilized L-aspartate ammonia-lyase from *Bacillus* sp. YM55-1 as biocatalyst for highly concentrated L-aspartate synthesis. *Bioprocess and Biosystems Engineering, 35*, 1437–1444.
11. Kisumi, M., Ashikaga, Y., & Chibata, I. (1960). Studies on the fermentative preparation of L-aspartic acid from fumaric acid. *Bulletin of the Agricultural Chemical Society of Japan., 24*, 296–305.
12. Tajima, T., Hamada, M., Nakashimada, Y., & Kato, J. (2015). Efficient aspartic acid production by a psychrophile-based simple biocatalyst. *Journal of Industrial Microbiology & Biotechnology, 42*, 1319–1324.
13. Kawabata, N., Hatanaka, H., & Odaka, H. (1995). Continuous production of L-aspartic acid from ammonium fumarate using immobilized cells by capture on the surface of nonwoven cloth coated with a pyridinium-type polymer. *Journal of Fermentation and Bioengineering, 79*, 317–322.
14. Chao, Y., Lo, T., & Luo, N. (2000). Selective production of L-aspartic acid and L-phenylalanine by coupling reactions of aspartase and aminotransferase in *Escherichia coli*. *Enzyme and Microbial Technology, 27*, 19–25.
15. Vargas, E., Ruiz, M. A., Ferrero, F. J., Campuzano, S., Ruiz-Valdepeñas Montiel, V., Reviejo, A. J., & Pingarrón, J. M. (2016). Automatic bionalyzer using an integrated amperometric biosensor for the determination of L-malic acid in wines. *Talanta, 158*, 6–13.
16. Monošík, R., Stred'anský, M., Greif, G., & Šturdík, E. (2012). Comparison of biosensors based on gold and nanocomposite electrodes for monitoring of malic acid in wine. *CEJC, 10*, 157–164.
17. Miertuš, S., Katrlík, J., Pizzariello, A., Stred'anský, M., Švitel, J., & Švorc, J. (1998). Amperometric biosensors based on solid binding matrices applied in food quality monitoring. *Biosensors & Bioelectronics, 13*, 911–923.
18. Gajovic, N., Warsinke, A., & Scheller, F. W. (1998). A bienzyme electrode for L-malate based on a novel and general design. *Journal of Biotechnology, 61*, 129–133.
19. Prodromidis, M. I., Tzouwara-Karayanni, S. M., Karayannis, M. I., Vadgama, P., & Maines, A. (1996). Amperometric determination of L-malic acid in a flow injection analysis manifold using packed-bed enzyme reactors. *Analyst, 121*, 435–439.
20. Mundaca-Uribe, R., Valencia-Muñoz, D., Castillo Felices, R., Neira Hinojosa, J., Aranda Bustos, M., & Peña-Farfal, C. (2017). Bienzymatic biosensor for malic acid based on malate dehydrogenase and transaminase immobilized onto a glassy carbon powder/carbon nanotubes/NAD^+ composite electrode. *Electroanalysis, 29*, 238–243.
21. Atci, E., Babauta, J. T., Ha, P. T., & Beyenal, H. (2017). Fumarate microbiosensor for use in biofilms. *Journal of the Electrochemical Society, 164*, 3058–3064.
22. Si, R.-W., Zhai, D.-D., Liao, Z.-H., Gao, L., & Yong, Y.-C. (2015). A whole-cell electrochemical biosensing system based on bacterial inward electron flow for fumarate quantification. *Biosensors & Bioelectronics, 68*, 34–40.
23. Villarta, R. L., Palleschi, G., Lubrano, G. J., Suleiman, A. A., & Guilbault, G. G. (1991). Amperometric aspartate electrode. *Analytica Chimica Acta, 245*, 63–69.
24. Palleschi, G., Lavagnini, M., Compagnone, D., Bertocchi, P., & Moscone, D. (1992). Flow monitoring of glutamate and aspartate in foods and pharmaceutical products with immobilized bienzyme electrochemical cells. *Electroanalysis, 4*, 851–857.
25. Campanella, L., Aturki, Z., Sammartino, M. P., & Tomassetti, M. (1995). Aspartate analysis in formulations using a new enzyme sensor. *Journal of Pharmaceutical and Biomedical Analysis, 13*, 439–447.
26. Kobos, R. K., & Rechnitz, G. A. (1978). Regenerable bacterial membrane electrode for L-aspartate. *Analytical Letters, 10*, 751–758.

27. Fatibello-Filho, O., Suleiman, A., & Guibault, G. G. (1989). Enzyme electrode for the determination of aspartate. *Biosensors, 4*, 313–321.
28. Aboulnaga, E.-H., Pinkenburg, O., Schiffels, J., El-Refai, A., Buckel, W., & Selmer, T. (2013). Effect of an oxygen-tolerant bifurcating butyryl coenzyme A dehydrogenase/electron-transferring flavoprotein complex from Clostridium difficile on butyrate production in *Escherichia coli*. *Journal of Bacteriology, 195*, 3704–3713.
29. Asano, Y., Kira, I., & Yokozeki, K. (2005). Alteration of substrate specificity of aspartase by directed evolution. *Biomolecular Engineering, 22*, 95–101.
30. Pilas, J., Iken, H., Selmer, T., Keusgen, M., & Schöning, M. J. (2015). Development of a multi-parameter sensor chip for the simultaneous detection of organic compounds in biogas processes. *Physica Status Solidi A: Applications and Materials Science, 212*, 1306–1312.
31. Kirchner, P., Reisert, S., Pütz, P., Keusgen, M., & Schöning, M. J. (2012). Characterisation of polymeric materials as passivation layer for calorimetric H_2O_2 gas sensors. *Physica Status Solidi A: Applications and Materials Science, 209*, 859–863.
32. Swain, G. M. (2007). Solid electrode materials: Pretreatment and activation. In C. G. Zoski (Ed.), *Handbook of electrochemistry* (pp. 111–153). Amsterdam: Elsevier.
33. Migneault, I., Dartiguenave, C., Bertrand, M. J., & Waldron, K. C. (2004). Glutaraldehyde: behavior in aqueous solution, reaction with proteins, and application to enzyme crosslinking. *Biotechnology Techniques, 37*, 790–802.
34. Broun, G. B. (1976). Chemically aggregated enzymes. In K. Mosbach (Ed.), *Methods in enzymology* (pp. 263–280). New York: Academic Press.
35. Chui, W. K., & Wan, L. S. C. (1997). Prolonged retention of cross-linked trypsin in calcium alginate microspheres. *Journal of Microencapsulation, 14*, 51–61.
36. Chakraborty, S., Sakka, M., Kimura, T., & Sakka, K. (2008). Characterization of a dihydrolipoyl dehydrogenase having diaphorase activity of *Clostridium kluyveri*. *Bioscience, Biotechnology, and Biochemistry, 72*, 982–988.
37. Massey, V. (1953). Studies on fumarase. II. The effects of inorganic anions on fumarase activity. *The Biochemical Journal, 53*, 67–71.
38. Ma, L., Cao, S.-G., Yan, B.-X., Zuo, H.-T., Ding, Z.-T., Meng, W.-F., & Cheng, Y.-H. (1992). Induced rebuilding of aspartase conformation. *Annals of the New York Academy of Sciences, 672*, 60–65.
39. Rudolph, F. B., & Fromm, H. J. (1971). The purification and properties of aspartase from *Escherichia Coli*. *Archives of Biochemistry and Biophysics, 147*, 92–98.
40. Rhee, J. I., & Sohn, O. J. (2003). Flow injection system for on-line monitoring of fumaric acid in biological processes. *Analytica Chimica Acta, 499*, 71–80.
41. Saribas, A. S., Schindler, J. F., & Viola, R. E. (1994). Mutagenic investigation of conserved functional amino acids in *Escherichia coli* L-aspartase. *The Journal of Biological Chemistry, 269*, 6313–6319.